TEMC-417-2024.R1

A Method for In-Situ Characterization of Human-Induced ESD

Gabriel Fellner, Simon Buttinger, David Pommerenke, *Fellow, IEEE*, Satyajeet Shinde, Michael Hillstrom

***Abstract*— The probability of electronic products being affected by electrostatic discharge (ESD) depends on the probability of the device being subjected to ESD and the voltage level. By determining this statistical probability, product risk assessment and the selection of appropriate ESD test levels can be performed to ensure the targeted field reliability is reached. Obtaining the necessary statistical information about ESD requires methods that can detect and quantify its parameters. Traditional ESD detection methods are predominantly stationary, requiring reference potential, and lack adaptability for portable devices and wearables. This paper demonstrates a novel, portable in-situ detection method based on on-body electric and magnetic field measurements. The proposed method integrates a wearable ESD sensor, capable of detecting discharge events, estimating voltage and current levels, and differentiating between human skin and human metal discharges. This sensor's design allows the characterization of the complex ESD environments of a person, offering a significant improvement over existing methods. Additionally, integration with a mobile application enables detailed analysis of the discharge scenario through user questionnaires for the first time.**

Index Terms*— Electrostatic discharge, electrostatic interference, in-situ measurement, ESD detection, risk assessment, threat assessment.

I. INTRODUCTION

As electrostatic discharges (ESD) have the potential to disrupt or even permanently damage electronic devices and components, it is essential to understand the risk posed by these events. Therefore, the IEC 61000-4-2 [1] regulatory framework describes a measurement setup which is used to test the ESD robustness of electronic devices. Depending on the product category, requirements on minimum robustness are also defined. An analysis of the FDA database in [2] revealed that even for ESD-compliant medical devices, ESD failures occur in the field. In order to ensure high field reliability, test levels exceeding the minimum requirement can be selected. To achieve a good balance between the cost of ESD protection and the reliability of the product, it is essential to determine the ESD threat for the device.

The majority of traditional ESD detection methods, such as charge voltage measurement and discharge current measurement, rely on stationary systems and reference potentials, prohibiting their applicability in dynamic environments. In [3], Wan et. al. analyzed walking voltages for various combinations of footwear and flooring materials. Charge voltages resulting from activities such as standing up from a chair or removing a sweater have been reported in [4] and the voltage after exiting a car seat in [5] and [6]. The characterization of specific tasks and materials, facilitates the understanding of potential risk for a product in a certain environment. However, as only charge voltages are measured, information on the occurrence and voltage level distribution of actual ESDs cannot be derived. Different studies have been conducted to obtain this information. Simonic in [7] and [8] used a current transformer to measure the ESD current of human- and furniture-induced ESD. In [9], Frei used field probes to capture radiated field of ESD events. Information obtained from the measurement of radiated fields can be used to characterize indirect ESD, but it is challenging to correlate this data with discharge currents or charge voltages.

The ongoing trend towards portable and wearable electronic devices also brings new challenges for ESD on these products, as previously described in [10]. A portable detection method is needed to characterize this complex and dynamic ESD environment. Portability allows to characterize the ESD threat across a mixture of environments and daily activities of people. Environments of people vary in flooring material, shoe material, material of frequently used tools or furniture, but also in ambient temperature and humidity. Activities such as frequent standing up from a chair, cloth removal or exiting a car can significantly influence the probability for high ESD voltage levels. Using a wearable detector, increases the usability for the participants, as ESD events are automatically monitored without requiring actions of a participant. In this paper, the authors' concept of a wearable ESD sensor, with the concept initially presented in [11], is subject to a comprehensive analysis. A comprehensive analysis of the on-body electric and magnetic fields is performed across different scenarios enabling judgement on the accuracy of on-body field measurement for ESD detection. Methods for utilizing this data to estimate ESD charge voltage and discharge current are presented, along with a novel wearable sensor device that integrates all these functionalities for the first time. The device allows for the

The financial support by the Austrian Federal Ministry for Digital and Economic Affairs, the National Foundation for Research, Technology and Development, and the Christian Doppler Research Association is gratefully acknowledged. *(Corresponding author: Gabriel Fellner)*

Gabriel Fellner is with the Institute of Electronics and Christian Doppler Laboratory for EMC Aware Robust Electronic Systems, Graz University of Technology, 8010 Graz, Austria (e-mail: gabriel.fellner@tugraz.at).

Simon Buttinger is with the Institute of Electronics, Graz University of Technology, 8010 Graz, Austria (e-mail: simon.buttinger@tugraz.at).

David Pommerenke is with the Institute of Electronics and Christian Doppler Laboratory for EMC Aware Robust Electronic Systems, Graz University of Technology, 8010 Graz, Austria (e-mail: david.pommerenke@tugraz.at).

Satyajeet Shinde is with Apple Inc., Cupertino, CA 95014 USA (e-mail: satyajeet_shinde@apple.com)

Michael Hillstrom is with Apple Inc., Cupertino, CA 95014 USA (e-mail: michael_hillstrom@apple.com)

detection of ESD events induced by an individual, estimation of voltage and current levels, and determination of whether the discharge was a human skin discharge or with a metal object. This method may be the most suitable for overcoming limitations to specific environments present in other methods. Potentially the device will be used in participant studies to collect statistical information on ESD for participants performing their daily activities.

II. Human-Induced ESD Occurrence and Severity Detection Methods

Several methods have been established to collect information on the occurrence and severity of ESD events. Each method has its own strengths and weaknesses. This section presents the most appropriate methods for collecting statistical information about human induced ESD.

A. Direct Voltage Measurement

Since the most commonly used parameter to rate ESD or define test levels is charge voltage, the most direct approach is direct voltage measurement. Direct measurement provides high accuracy and reduces uncertainties due to conversion, for example from discharge current to voltage level. In order to measure the voltage between a person and ground, this method requires ground as a reference potential and therefore prohibits its application in portable detection systems. Many studies have been conducted on charging levels in certain scenarios or material combinations using direct voltage measurement. In [5], [6] for persons after exiting a car, in [3], [12], [13] after walking on different floors, in [4], [14] after standing up from a chair or removing a sweater.

Commercial contact and non-contact voltmeters are available for the measurements. For example the ESDEMC ES105 contact voltmeter or Trek 347 non-contact voltmeter.

It should be mentioned that measurement of charge voltage is only possible prior to the discharge event itself, since during the ESD the voltage is reduced by voltage-dividing effects between the source, spark and target impedance. This means that the method is best suited for measuring body voltage before certain objects are touched, assuming that an ESD event would have occurred if the object had been touched.

B. Discharge Current Measurement

As discharge current is known to be a crucial parameter for upsetting or damaging electronics, the measurement of discharge current can provide deep insight into the severity of an ESD. This method can be used in specific objects/products for example by installing a current transformer or broadband shunt resistor. Measurement of discharge current also makes it possible to determine the occurrence of a discharge event. The measurement itself has demanding requirements on the bandwidth of the equipment, thus ESD currents can reach frequencies beyond 1 GHz, especially for human-metal discharges and low-voltage air discharges [15].

The method has been used by Simonic in [7] and [8]. Commercial current clamps such as the Fischer F-65, a current target as in [1] and [16], or a 1Ω disk resistor as in [17] can be used in combination with fast acquisition instruments.

C. On-Body Electric-Field Measurement

People carrying static charges exhibit an electric field on their bodies. This electric field depends on the potential, the geometry at the location on the body, and the distance/geometry of the surrounding environment. This means that if certain assumptions are made about the environment in the vicinity of the field measurement location, the charge voltage of a person can be estimated, such a method has been presented in [10], [18]. Further this method allows the detection of discharge events by detecting a rapid collapse of the electric field on the body, as demonstrated in [11]. Information on the accuracy of this method is not available as a comprehensive analysis has not been published yet. This paper will show that the accuracy suffers from the assumptions about the sensor environment needed to relate field strength to charge voltage, but can be improved by measuring field strength at multiple locations on the body. A major benefit of this method is that no reference potential is needed, so that it can also be used in portable systems.

Currently the only commercial product available is the StatIQ Band from Ionatech, which aims to improve ESD mitigation in manufacturing processes by measurement of the electric field at the upper arm.

D. Radiated Field Measurement

Not only can ESD disrupt or damage devices when applied directly, but the radiated fields caused by the rapid change in current and potential can reach field strengths of several kV/m [15], [19]. The radiated fields can be monitored using antennas. While this method does not allow the observation of direct ESD on a product, it can be used as a supporting method to characterize the overall electromagnetic environment. For example, a measurement system could be placed in various locations similar to the location of the product in the application, as in [9], [20]. Measurement of radiated fields is also a common method to detect ESD in manufacturing environments. Multiple antennas can be used to localize the event based on multilateration, as in [21] and [22], or based on cross-correlation with simulation data, as in [23].

E. Comparison

A comparison of the different detection methods is presented in Table I. Direct voltage measurement is the most used method to determine charge voltage levels, but has major limitations, as it cannot detect actual ESD events and therefore their occurrence rate. Further a reference potential is required prohibiting portable operation. Measurement of the discharge current has the advantage, that the actual ESD event happened and is detected. Therefore the occurrence rate can be determined, also portability is possible but has not been implemented in a device or study according to the knowledge of the authors of this paper. Measurement of the on-body electric field for ESD event detection, has many advantages for measuring occurrence, charge and ESD voltage and further can be used portable without reference potential. The In-Situ detection system presented in this paper combines discharge current measurement and on-body electric field measurement, by the usage of electromagnetic field sensors.

TABLE I
Comparison of ESD Detection Methods

	Direct voltage measurement	Discharge current measurement	On-Body electric field measurement	In-Situ Detector
ESD current	✗	✓	✗	✓
ESD voltage	✗	✗	✓	✓
Charge voltage	✓	✗	✓	✓
Occurrence	✗	✓	✓	✓
Portable possible	✗	(✓)	✓	✓
Accuracy	High	High	Med.	Med.

III. In-Situ ESD Measurement System

A. System Architecture

The ESD event detection principle based on the on-body electric field, as presented in [11], has been enhanced and integrated into a novel fully portable measurement device, as illustrated in Fig. 1(a). The device is capable of detecting ESD by measuring changes in a person's electric field and recording the amplitude of the field strength. Additionally, a magnetic field sensor has been incorporated to capture information related to the discharge current when located near the main discharge current path. The device employs a humidity and temperature (H&T) sensor to measure the humidity of the environment. The sensor is necessary because ESD occurrence is dependent on humidity. The data collected by the device is transferred to a smartphone via Bluetooth Low Energy (BLE). As the device is intended to be used for collecting statistical data on ESD with a large number of study participants, usability and comfort were also of concern in the design. Therefore, the device has the form factor of a large smartwatch and a battery life of more than one day, so that it will be recharged overnight. This novel device combines on-body electric field measurement for human induced ESD event detection, voltage level estimation and current estimation. Herby closing the gap between individual detection methods presented in the previous section.

The block diagram in Fig. 2 illustrates the various features of the sensor device. The device is charged via a micro USB port, with the battery management unit (BMU) responsible for charging the battery and supplying the microcontroller unit (MCU) and power management integrated circuit (PM-IC). The PM-IC provides +5 V and -4 V for the analog peak detect and hold (PDH) circuit. The device employs a push button as the user interface for power on/off and BLE visibility (advertising) control. Optical and acoustic feedback is provided by an onboard buzzer and LED, which signalize power status changes. The electric field sensor is connected to a high impedance buffer amplifier, which is followed by the internal analog to digital converter (ADC) of the MCU. As the magnetic field sensor delivers pulsed signals with a narrow pulse width in the range of 3 ns, an analog peak-hold circuit is employed to hold the peak value for a duration of multiple hundred microseconds [24]. The almost constant output signal can then be sampled using the slow ADC of the MCU, which operates at 160 kSa/s. As the PDH circuit requires up to 35 mA from the battery, continuous operation would result in a battery life of less than one day when using a small 450 mAh lithium polymer (LiPo) cell. To address this, the PDH circuit is deactivated when there is no motion and reactivated as soon as any motion is detected. This approach assumes that an ESD event on the hand can only be caused by moving towards an object. For instance, approaching an object with the hand. This configuration enables the reduction of power consumption, thereby extending the battery life to at least one day.

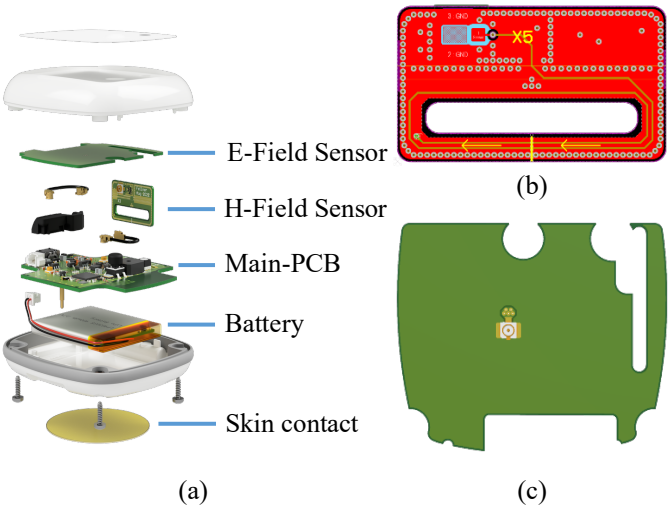

Fig. 1. In-Situ ESD measurement system (a) Structure of the sensor highlighting key components (b) PCB layout of the magnetic field sensor (c) Rendering of the 2-layer electric field sensor PCB.

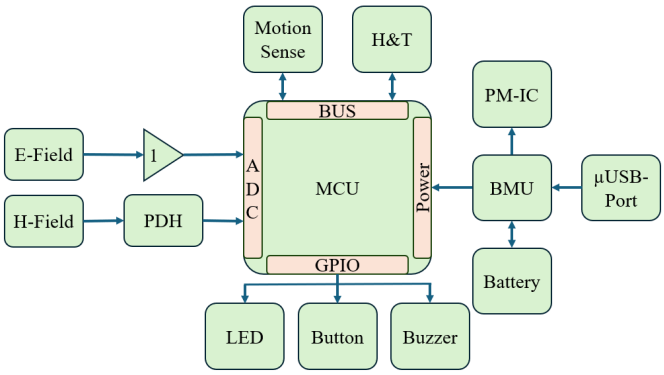

Fig. 2. Simplified block diagram of the in-situ ESD detector. H&T: humidity and temperature sensor, PDH: peak detect and hold, PM-IC: power management IC, BMU: battery management unit.

B. Electric Field Measurement

The sensor depicted in Fig. 1 (c) is an electric field sensor known as a D-dot sensor. A two-layer printed circuit board

(PCB) is used, where one layer serves as an electrode and the other layer is ground. In the presence of an electric field, it generates an output current that is proportional to dD/dt. To obtain the field strength, the signal must be integrated, which can be achieved through either digital or analog signal processing. The transfer characteristic of this type of sensor can be altered by the loading condition. Beyond a certain corner frequency the derivative behavior is compensated by a low-pass network formed by the intrinsic capacitance of the sensor and the load impedance. This technique is commonly known as "self-integration" and described in more detail in [25]. The corner frequency also determines the decay time of the step response. Fig. 3 shows the schematic of the interface for the electric field sensor. By biasing the sensor electrode with VDD/2, positive and negative changes can be measured using the ADC of the MCU. The load capacitance C_S determines the sensitivity of the sensor, while the load impedance sets the time constant, which is given by $\tau = R_B/2 \cdot C_S$. The final sensor, constructed using the values presented in Fig. 3, exhibits a lower corner frequency of approximately 12 Hz. This frequency is sufficiently low to enable readout using a slow ADC.

In order to get accurate sensor responses, a skin-contact PCB is installed on the bottom side of the sensor device. This PCB ensures that the system ground is on the same potential as the body of the person. An ohmic connection might be the best option, although a defined capacitive coupling for example with a coated PCB also enables accurate functionality.

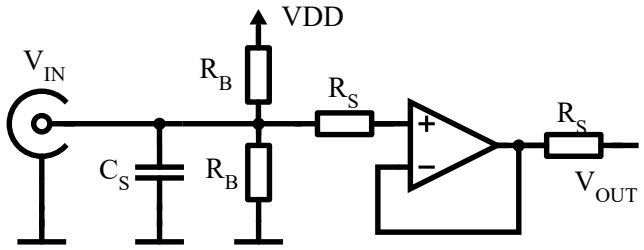

Fig. 3. Schematic of E-field sensor interface. Voltage follower circuit with component values: $C_S = 2.68\ nF$, $R_B = 10\ M\Omega$ and $R_S = 10\ k\Omega$.

C. Magnetic Field Measurement

Fig. 1 (b) depicts the magnetic field sensor which is integrated into the device. The sensor is based on a two-turn loop structure and has ground shielding layers to reduce unintentional electric field coupling. The use of two turns in combination with a large loop area of 47 mm² results in a reasonable sensitivity. This also simplifies the application of the self-integration principle to the B-dot sensor. With a load resistance of 50 Ω which is the input impedance of the peak detector, a corner frequency of 80 MHz is reached while maintaining good sensitivity. Due to the narrow width of the initial peak of ESD currents, which can be shorter than 3 ns, the field sensor produces a response with a similar short pulse width. To capture the peak value of this fast response, an ADC with a sampling rate of at least 500 MSa/s and signal processing hardware capable of processing the data stream at high speeds would be required. However, such high speeds typically result in high power consumption, making them unsuitable for small battery-powered devices. To determine the peak value of the sensor response without significantly reducing battery life, we use an analog peak detect and hold (PDH) circuit, which has been presented in [24]. A high-level schematic is shown in Fig. 4, where a high-speed operational transconductance amplifier (OTA) is used in conjunction with a rectifying common base npn-transistor to charge a capacitor. This capacitor is capable of holding the peak value of the input signal for multiple hundred microseconds. The OTA is constructed from fast discrete bipolar transistors and the fast buffer using a n-channel JFET. The circuit is capable of detecting these pulses with a dynamic range of 37 dB. While the polarity of the magnetic field sensor response is determined by the direction of the discharge current, the PDH circuit is only able to detect positive pulses. If the probability for positive and negative ESD events is equal, information on the discharge current would only be available for 50 % of the discharges.

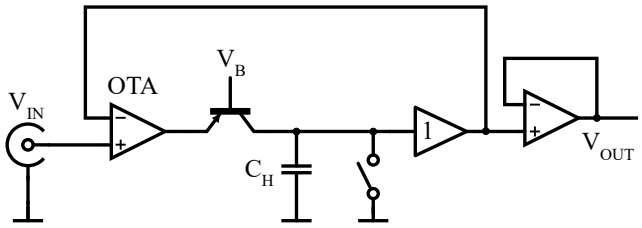

Fig. 4. High-level schematic of PDH circuit from [24], with the OTA and buffer built from discrete components.

IV. ESD Detection via On-Body Electric Field

A. ESD Event Detection

The on-body electric field is proportional to and varies with the changing potential of the body. There are multiple reasons for these changes in the potential:

- Triboelectric charging
- Slow discharge via resistive path to GND
- Charge compensation from ions in the air
- Movement that changes the surroundings, like walking through a door path (capacitance variation)
- Actual ESD

Fig. 5 (a) illustrates the on-body electric field to the surroundings and Fig. 5 (b) depicts the qualitative nature of the on-body electric field before and after an ESD to ground. The inherent speed of the discharge event can be utilized to identify the occurrence of an ESD as demonstrated in Fig. 5 (c).

On the MCU, this detection method is implemented by continuously calculating the difference between two samples, which is proportional to the derivative of the sensor signal since the sampling interval is constant. If this difference exceeds the set threshold value, it is considered as ESD event, and the amplitude of the electric field sensor and magnetic field sensor responses are extracted as parameters of the ESD.

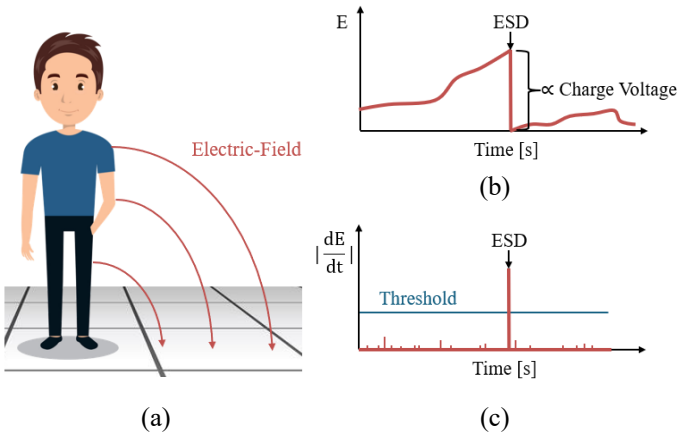

Fig. 5. (a) Person with on-body electric field lines (b) Principle of on-body electric field before and after an ESD (c) Method to identify ESD event in electric field.

B. Field Strength Dependencies and Voltage Level Estimation

The field strength on the body depends on several parameters, including:

- Body voltage
- Location on body
- Vicinity to conductive objects in the surrounding
- Posture of the person

Therefore, in order to relate field strength to body voltage, assumptions must be made for the other parameters. The location of the field measurement is typically known and fixed. However, the person's posture and proximity to conductive objects vary over time. To analyze the effect of the person's posture and proximity to conductive objects, an electrostatic simulation was performed using CST Microwave Studio [26]. Fig. 6 (a) shows the postures of the person used to simulate the electric field at the wrist and shoulder locations. The corresponding simulation result is shown in Fig. 6 (b), where the field strength is normalized to posture 2, which is considered to be the most common discharge gesture when reaching for an object. At the wrist location, the variation across postures is in the range of ±10 %. In contrast, at the shoulder location, a worst-case error of -30 % is observed in posture 4. Fig. 6 (c) shows the normalized field strength versus distance to a perfectly electric conducting (PEC) wall on the side of the electric field measurement. For distances greater than 0.5 m, the change is relatively uncritical. However, towards 0.1 m, the error can exceed several times 100 %.

For a known location on the body and a distance greater than 0.5 m from conductive objects, the charge voltage level can be estimated using the following equation:

$$V_{charge} = E \cdot CF_E \tag{1}$$

In this equation V_{charge} represents the charge voltage of the person, E is the electric field strength at the body location, and CF_E is the calibration factor which relates field strength to charge voltage in the described scenario. It is crucial to recognize that this calibration factor is only precise within the context for which it was derived. In particular, if the distance to metallic objects is less than 0.5 m, the elevated field strength would result in a significant overestimation of charge voltage. To mitigate the likelihood of overestimation due to proximity to conductive objects, the electric field can be measured at different locations on the body. The estimated charge voltage is then calculated by combining the two electric field measurements using a minimum function. It is assumed that the lower value of the voltage level estimation is farther away from any metal, thus approximating the calibration scenario more closely.

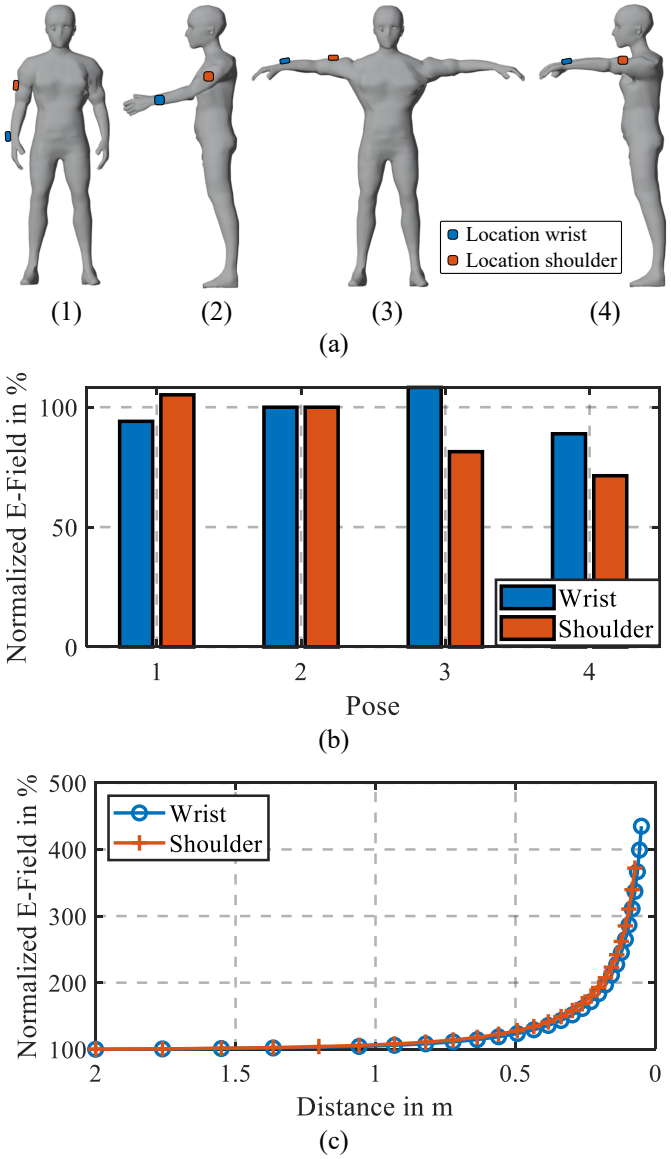

Fig. 6. (a) Postures used for simulation of on-body electrostatic field strength. (b) Simulation result of electric field at wrist and shoulder (upper arm) location (c) Simulated increase in electric field when approaching PEC wall on sensor side for wrist and shoulder location in posture 1.

C. Consecutive Discharges

As discussed in [27], air-discharge ESD events typically consist of multiple successive discharges. The time intervals between these pulses can be as short as 10 µs or as long as multiple hundred milliseconds. One potential explanation for this phenomenon is that the arc quenches when its current is

insufficient to sustain air ionization. As the finger approaches the electrode, the energy required to initiate a spark decreases, allowing the spark to be reignited. This procedure can repeat until the individual is fully discharged.
Such consecutive discharges are also evident in the electric field on the body of a person that is subject to an ESD. Fig. 7 shows the sensor response of an electric field sensor to an ESD at different charge voltages. The waveforms exhibit multiple steps, while the delay and amplitude of the consecutive event increase with voltage level. While each of these consecutive discharges is detected individually by the measurement device, they are treated as a single event consisting of multiple pulses. The summation of the individual pulses of an event then gives the charge voltage of the person, as the person is discharged in multiple steps. The events are considered a consecutive if they take place within 50 ms, as within this time recharging and a second contact is unlikely.

D. Calibration of Electric Field System Factor

Equation (1) relates the on-body electric field to body charge voltage. By means of calibration, the calibration factor CF_E can be replaced by a system factor. For calibration purposes, we have selected normal standing and reaching for an object (pose 2 in Fig. 6 (a)) without any nearby metallic objects as the scenario. In order to calibrate the system, a person wearing the sensor is charged to known voltage levels (ranging from 1.5 kV to 12 kV) and causes an ESD by touching a small grounded metallic plate. During the procedure, the sensor response is recorded, and the system factor is calculated as the charge voltage divided by the sensor response. This is given by the following equation:

$$SF_E = \frac{V_{charge}}{\hat{V}_{sensor}} \tag{2}$$

With SF_E as system factor, with V_{charge} representing the charge voltage of the person, and $\hat{V}_{sensor}$ representing the peak value of the electric field sensor. For consecutive discharge events, $\hat{V}_{sensor}$ is the sum of the individual consecutive amplitudes. The resulting sensor responses for different charge voltage levels are shown in Fig. 7. From this procedure the system factor is determined to a value of 25 kV/V for the wrist sensor and 26 kV/V for the shoulder sensor. Further, a value of 120 V is added to compensate for systematic offset in the system. The charge voltage and measurement of the sensor response during the calibration is very accurate. The main uncertainty comes from the variation in the electric field caused by the dependency on the posture as shown in Fig. 6 (b). To minimize this uncertainty during calibration, multiple discharges per voltage level are recorded and the results are averaged.

V. Estimations of Discharge Current

A. Magnetic Field Around Wrist

In an ESD event being triggered by contact with an object with the hand, the majority of the discharge current flows through the hand and wrist. The initial peak of an ESD current does not pass the wrist region, since the current comes from displacement currents of the local capacitance of the hand. This flow of current results in the generation of a magnetic field around the wrist, which is proportional to the discharge current. The magnetic field can be approximated for a round wrist as follows:

$$H = \frac{i_{ESD\ Wrist}}{2\pi \cdot r} \tag{3}$$

Where H is the circular magnetic field around the wrist, $i_{ESD\ Wrist}$ is the discharge current passing the wrist and r is the distance from the center of the wrist to the location of the field measurement. When the magnetic field is measured right above the skin at the wrist, (3) shows that the measured field strength is expected to vary for wrists with different diameters. The average wrist circumference for males and females has been analyzed in [28] and is 17.42 cm ± 0.83 cm for males and 15.12 cm ± 0.69 cm for females. A range of 16.34 cm ± 1.91 cm includes more than one standard deviation between males and females. With the assumption of a round wrist, this range would result in variations of approximately ±11.5 %. By accepting this variation, the same calibration factor can be used to estimate the ESD current of different persons. The estimated discharge current is calculated using the following equation:

$$i_{ESD\ Wrist} = H \cdot CF_H \tag{4}$$

With $i_{ESD\ Wrist}$ as the discharge current to be estimated, H as magnetic field at the measurement location, and CF_H as a calibration factor which relates the magnetic field to the discharge current. As the initial peak of the current does not pass the wrist location, $i_{ESD\ Wrist}$ would not be the full discharge current.

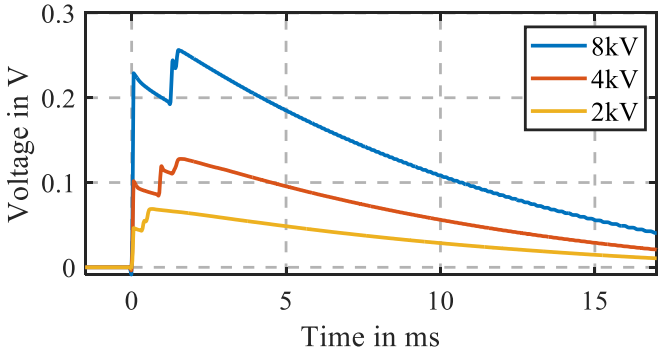

Fig. 7. Measured waveforms of electric field sensor at wrist location during calibration measurements. Person charged from 2 kV to 8 kV.

B. Calibration for Discharge Current System Factor

The use of a B-dot sensor with self-integration allows for a flat frequency response, above 80 MHz. This enables the use of a constant system factor for the conversion from sensor voltage to discharge current, provided that the majority of the frequency spectrum exceeds this corner frequency. By means of calibration measurements, a system factor which relates peak sensor voltage to peak ESD current can be determined. Such a factor compensates for the blind current of the hand, which does not pass through the wrist. The system factor can thus replace the calibration factor from (4) and is given by:

$$SF_H = \frac{\hat{\imath}_{ESD}}{\hat{V}_H} \quad (5)$$

With SF_H as system factor of the magnetic field sensor, $\hat{\imath}_{ESD}$ as peak ESD current, and $\hat{V}_H$ as peak sensor response voltage. This system factor is determined by measuring the response of the magnetic field sensor while a person wearing the sensor on the wrist is charged to a high voltage and then touches an ESD current target. This is done directly with the finger or with a small piece of metal. An optical link with a bandwidth of 3 GHz from the field sensor to the oscilloscope allows for the analysis of the sensor response while the individual remains insulated from the ground. Fig. 8 illustrates the captured peak values from the magnetic field sensor versus the peak discharge current. The measurement results were generated using charge voltages ranging from 2 kV to 8 kV, with and without a piece of metal in the hand. The fit of a line to the data illustrates how well a system factor SF_H of 4.9 A/V can be used for the conversion. Deviations from the linear fit can be attributed to the finite lower corner frequency of the sensor and variation of the blind current before the wrist. The combination of the different charge voltages and metal object results in various different amplitudes for the discharge current. The nature of the air discharges leads to strong variations in rise times due to the spark.

C. Human Skin or Human Metal Discharge?

A human metal discharge, which is often referred to as a human metal model (HMM), is considerably more severe than a human skin discharge, which is modeled using the human body model (HBM). At a given voltage level, a HMM results in a significantly higher current than HBM. Since the voltage level can be estimated from the electric field, the estimation of the discharge current can be used to determine the type of discharge.

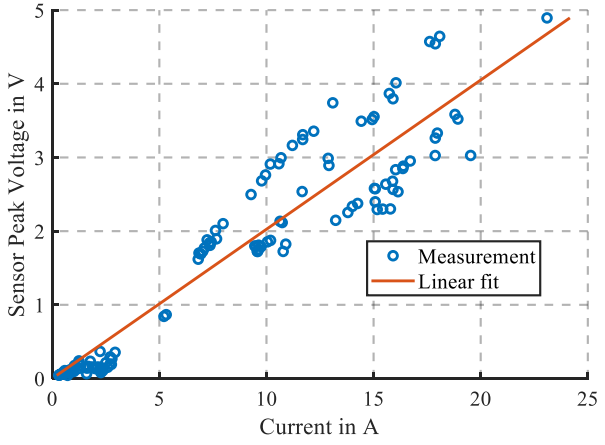

Fig. 8. Measured peak sensor response of the magnetic field sensor on the wrist of a person while discharging to an ESD current target. Charge voltages from 2 kV to 8 kV with human skin and human metal discharges.

To validate this hypothesis, measurements were performed for HMM and HBM discharges. Fig. 9 depicts the estimated peak discharge currents which were calculated by multiplying the magnetic field sensor response by the conversion factor SF_H for HMM and HBM discharges at different charge voltages. The results demonstrate that HBM discharges lead to rather small currents below 5 A, while almost all HMM discharges yield responses exceeding this value.

From the standard [29] the peak discharge current for HBM is 0.66 A/kV compared to 3.75 A/kV for HMM [1]. Nevertheless in the real application the discharges are air discharges with a spark resistance depending on environmental conditions, field strength and approach speed leading to deviating peak currents. Also the size of the metal piece for a HMM discharge influences the peak current as explained in [30]. In [31], 0.8 A/kV to 0.5 A/kV were reported for HBM discharges showing a decreasing trend for increasing voltage levels as the spark length increases. Because of this large range of peak discharge currents at HBM and HMM there is no ultimate unique solution to categorize ESD events as HBM or HMM. Rating events having currents higher than the 0.66 A/kV from the HBM standard as HMM would overestimate the majority of discharges in a similar way as considering events lower than 3.75 A/kV as HBM would underestimate.

For this application, the threshold used to distinguish HBM from HMM in the measurements was empirically determined from the measurements in Fig. 9. The threshold value is calculated for the different voltage levels as the mean between the maximum current for a HBM and minimum current of a HMM. This threshold value is visualized as red vertical line in the plot. To determine the ratio of occurrence between HMM and HBM, both must lead to a measurable sensor response across the measurement range. If no current was measured for an ESD event, it can be assumed that it did not originate from the hand equipped with the sensor. In the measurements, the minimum of the estimated discharge current in the measurement was 0.2 A and the system is capable of detecting even smaller currents, down to 0.1 A. The results demonstrated that the sensor's sensitivity makes it possible to distinguish HMM from HBM.

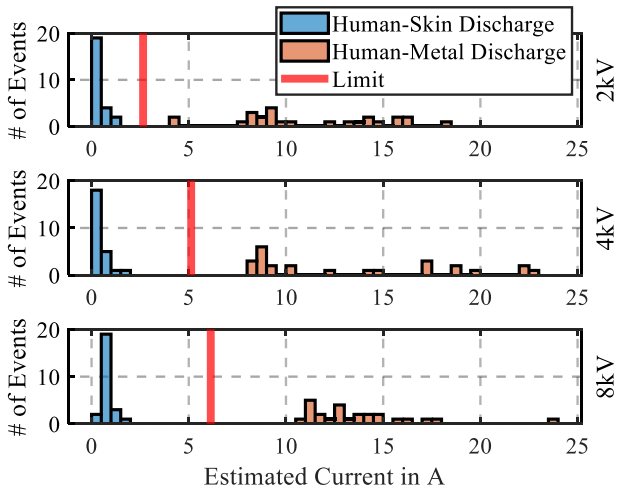

Fig. 9. Estimated discharge current from H-field sensor for HBM and HMM discharges. For HMM discharges an air discharge tip has been used.

VI. Sensor Applications

The in-situ ESD measurement system enables the collection of data on the occurrence rate and severity of human-induced ESD. It provides information such as the event rate (number of ESDs per hour), voltage and current level, and type of discharge, when a discharge occurred at the arm equipped with the sensor. One significant advantage of the system is its portability, which allows for monitoring ESDs during various activities and locations. The method described, overcomes the limitation of monitoring only a single room or product, allowing for a more comprehensive understanding of human-induced ESD. The concept for such a study is shown in Fig. 10, where participants would wear two sensor devices on opposite arms and the collected data would be transferred to the user's smartphone.

As data is transferred to a custom phone application, such a study can be supported by prompting users to answer a questionnaire when a discharge was detected. This questionnaire might address the following questions:

- What were you doing just before the ESD?
- What object did you touch during the ESD?
- Take a picture of the discharge scenario

If this additional information is collected from study participants, it is possible to identify possible charging mechanisms. Furthermore, the information about the object touched and the ESD occurrence can be related to certain devices or products.

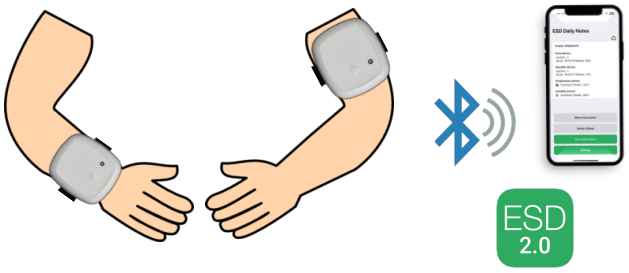

Fig. 10. ESD sensor arrangement on body including accessories. Data transfer using BLE to custom application running on smartphone.

VII. Discussion

The relationship between electric field strength on the body and charge voltages is subject to variation in different electrostatic environments. Local field strength may be increased by a nearby metallic object or, conversely, slightly decreased by a posture that shields the sensor with another body part. Both scenarios have the potential to result in estimation errors. The use of two sensor measurement locations effectively mitigates this variation in most cases, although it cannot be entirely eliminated. In a statistical approach, the risk of outliers can be accepted. For a quantitative analysis of individual events further information provided by the user can be used to ensure that the electric field was not artificially enhanced by nearby objects. Taking a picture of the discharge scenario in the mobile application would be such an option.

For the sensor located on the wrist, the magnetic field sensor response correlates well with the discharge current. Although some variation is present, the sensor can give reasonable estimates for the discharge current. Especially the blind current from the hand, which does not pass the wrist, contributes to this variation. For statistical analysis, this variation in current estimation may not have a significant influence as errors that are symmetrically distributed will average out.

VIII. Conclusion

The collection of statistical data on ESD requires the use of advanced detection methodologies. In particular, the increasing prevalence of portable devices and wearables necessitates the ability to detect ESD events in a portable manner, as also devices are not operated in a single environment anymore. The in-situ detection method presented here addresses critical gaps in existing methodologies for characterizing complex ESD environments with respect to event occurrence, charge voltage level estimation, discharge current estimation, and the determination of the discharge type. Electromagnetic simulations of the on-body electric field in different scenarios and postures of a person showed, that the wrist location is less sensitive to changes in posture. Simulations showed strong increase in the field strength for conductive objects in close vicinity, leading to errors in voltage level estimation. These results show the necessity to use multiple sensor locations to avoid overestimation based on local field enhancement by nearby objects. For the first time, the magnetic field around the wrist is shown to be able to be used for estimating the ESD current through this hand. Further the combination with the implemented voltage level estimation, allows to determine the type of the discharge event. The in-situ sensor device, along with its underlying methods, has the potential to be utilized in large-scale participant studies to effectively characterize ESD environments of interest. Data transfer to a custom mobile application allows for the addition of study participants as a source of information, thereby facilitating the collection of background information on the discharge event. The collection of such background information right after the occurrence of an ESD allows for the correlation of captured events to specific activities, environments, or objects. This provides information that would otherwise be immeasurable through conventional measurement techniques. The in-situ detector with its ability to monitor the ESD activity of a person across various environments has the potential to provide a comprehensive understanding of real-world ESD occurrence. Statistical results obtained with the in-situ detector together with a comprehensive comparison to other ESD statistics are presented in [32].

Acknowledgment

The authors would like to acknowledge the support from Matthias Wintersteller in performing calibration measurements.

References

[1] IEC 61000-4-2:2008, "Electromagnetic compatibility (EMC) - Part 4-2: Testing and measurement techniques - Electrostatic discharge immunity test," 2008.

[2] M. Kohani and M. Pecht, “Malfunctions of Medical Devices Due to Electrostatic Occurrences Big Data Analysis of 10 Years of the FDA’s Reports,” IEEE Access, vol. 6, pp. 5805–5811, 2018, doi: 10.1109/ACCESS.2017.2782088.

[3] F. Wan, D. Swenson, M. Hillstrom, and C. Stayer, “The effect of humidity on static electricity induced reliability issues of ICT equipment in data centers - Motivation and setup of the study,” ASHRAE Trans, 2013.

[4] A. Talebzadeh, M. Moradian, Y. Han, D. E. Swenson, and D. Pommerenke, “Electrostatic charging caused by standing up from a chair and by garment removal,” in 2015 IEEE Symposium on Electromagnetic Compatibility and Signal Integrity, IEEE, Mar. 2015, pp. 57–62. doi: 10.1109/EMCSI.2015.7107659.

[5] K. K. Katrak, “Human body electrostatic charge (ESC) levels: are they limited by corona bleed off or environmental conditions?,” in Electrical Overstress/Electrostatic Discharge Symposium Proceedings, IEEE, 1995, pp. 73–85. doi: 10.1109/EOSESD.1995.478270.

[6] B. Andersson, L. Fast, P. Holdstock, and D. Pirici, “Charging of a person exiting a car seat,” J Phys Conf Ser, vol. 142, p. 012004, Dec. 2008, doi: 10.1088/1742-6596/142/1/012004.

[7] Simonic R., “Personnel ESD statistics,” in IEEE/EMC Symposium, Boulder, USA, 1981.

[8] R. B. Simonic, “Electrostatic Furniture Discharge Event Rates for Metallic-Covered, Floor-Standing Information Processing Machines,” in IEEE International Symposium on Electromagnetic Compatibility, Santa Clara, USA: IEEE, Sep. 1982, pp. 1–8. doi: 10.1109/ISEMC.1982.7567744.

[9] Frei S., “The occurrence of transient fields and ESD in typical selected areas,” in Electromagnetic compatibility, Wrocław, Jun. 1998.

[10] N.-C. Lin, “Wearable and Wireless Human Body Electrostatic Monitoring System,” in 2015 International Conference on Intelligent Information Hiding and Multimedia Signal Processing (IIH-MSP), IEEE, Sep. 2015, pp. 53–56. doi: 10.1109/IIH-MSP.2015.68.

[11] G. Fellner et al., “Wearable ESD Occurrence Rate Detection with Voltage Level Estimation,” in 2022 International Symposium on Electromagnetic Compatibility – EMC Europe, IEEE, Sep. 2022, pp. 268–272. doi: 10.1109/EMCEurope51680.2022.9901093.

[12] H. Ryser, “The relationship between ESD test voltage and personnel charge voltage,” in EOS/ESD Symposium Proceedings, 1990.

[13] A. Talebzadeh, A. Patnaik, X. Gao, M. Moradian, D. E. Swenson, and D. Pommerenke, “Dependence of ESD charge voltage on humidity in data centers: Part II - Data analysis,” ASHRAE Trans, pp. 37–48, 2015.

[14] A. Talebzadeh, M. Moradian, Y. Han, A. Patnaik, D. E. Swenson, and D. Pommerenke, “Dependence of ESD charge voltage on humidity in data centers: Part I - Test methods,” in ASHRAE Transactions, 2015, pp. 58–70.

[15] D. Pommerenke, “ESD: transient fields, arc simulation and rise time limit,” J Electrostat, vol. 36, no. 1, pp. 31–54, Nov. 1995, doi: 10.1016/0304-3886(95)00033-7.

[16] G. Fellner, D. Pommerenke, L. Zeitlhoefler, and F. Zur Nieden, “Transmission Line Based CDM ESD Current Target to Overcome Bandwidth Limitations,” in 2024 International Symposium on Electromagnetic Compatibility – EMC Europe, IEEE, Sep. 2024, pp. 640–645. doi: 10.1109/EMCEurope59828.2024.10722655.

[17] H. Rezaei, M. Drallmeier, J. R. Floyd, W. Huang, D. Beetner, and D. Pommerenke, “1 Ω Disk Resistor Full-Wave Modeling for JS-002 Standard,” in 2021 43rd Annual EOS/ESD Symposium (EOS/ESD), IEEE, Sep. 2021, pp. 1–10. doi: 10.23919/EOS/ESD52038.2021.9574740.

[18] S. Yong, A. Hosseinbeig, S. Yang, M. B. Heaney, and D. Pommerenke, “Noncontact Human Body Voltage Measurement Using Microsoft Kinect and Field Mill for ESD Applications,” IEEE Trans Electromagn Compat, vol. 61, no. 3, pp. 842–851, Jun. 2019, doi: 10.1109/TEMC.2018.2836869.

[19] G. Fellner, A. Pak, S. M. Mousavi, C. Koger, A. Khorrami, and D. Pommerenke, “Quantification of ESD Pulses Caused by Collision of Objects,” in 2022 International Symposium on Electromagnetic Compatibility – EMC Europe, Gothenburg, Sweden: IEEE, Sep. 2022, pp. 273–278. doi: 10.1109/EMCEurope51680.2022.9901123.

[20] T. Takai, M. Kaneko, and M. Honda, “One of the methods of observing ESD around electronic equipments,” in Proceedings Electrical Overstress/Electrostatic Discharge Symposium, ESD Assoc, 1996, pp. 186–192. doi: 10.1109/EOSESD.1996.865141.

[21] D. L. Lin, L. F. DeChiaro, and M.-C. Jon, “A Robust ESD Event Locator System With Event Characterization,” in Proceedings Electrical Overstress/Electrostatic Discharge Symposium, IEEE, 1997, pp. 88–98. doi: 10.1109/EOSESD.1997.634230.

[22] J. Bernier, G. Croft, and R. Lowther, “Esd Sources Pinpointed By Analysis Of Radio Wave Emissions,” in Proceedings Electrical Overstress/Electrostatic Discharge Symposium, IEEE, 1997, pp. 83–87. doi: 10.1109/EOSESD.1997.634229.

[23] G. Fellner, A. Pak, and D. Pommerenke, “Detection and Localization of CDM like ESD using a novel Sensor derived from Leaky-Coax,” in 2023 International Symposium on Electromagnetic Compatibility – EMC Europe, Krakow, Poland: IEEE, Sep. 2023, pp. 1–6. doi: 10.1109/EMCEurope57790.2023.10274257.

[24] G. Fellner et al., “Nanosecond Peak Detect and Hold Circuit With Adjustable Dynamic Range,” IEEE Trans Instrum Meas, vol. 72, pp. 1–8, 2023, doi: 10.1109/TIM.2023.3289555.

[25] R. J. Spiegel, C. A. Booth, and E. L. Bronaugh, “A Radiation Measuring System with Potential Automotive Under-Hood Application,” IEEE Trans Electromagn Compat, vol. EMC-25, no. 2, pp. 61–69, 1983, doi: 10.1109/TEMC.1983.304149.

[26] “CST Microwave Studio.”

[27] R. C. Pepe, “ESD multiple discharges,” in IEEE 1991 International Symposium on Electromagnetic Compatibility, Cherry Hill, NJ, USA: IEEE, 1991, pp. 253–258. doi: 10.1109/ISEMC.1991.148229.

[28] C. Gordon et al., “Anthropometric Survey of U.S. Army Personnel: Summary Statistics, Interim Report for 1988,” Yellow Springs, Ohio, USA, 1989.

[29] IEC 60749-26, “Semiconductor devices - Mechanical and climatic test methods - Part 26: Electrostatic discharge (ESD) sensitivity testing - Human body model (HBM),” 2018.

[30] D. Pommerenke and M. Aidam, “ESD: waveform calculation, field and current of human and simulator ESD,” J Electrostat, vol. 38, no. 1–2, pp. 33–51, Oct. 1996, doi: 10.1016/S0304-3886(96)00028-9.

[31] N. Becanovic, G. Fellner, S. Buttinger, and D. Pommerenke, “Modified ESD Generator to Emulate Body Worn Equipment ESD and Human Skin ESD,” in 2023 International Symposium on Electromagnetic Compatibility – EMC Europe, IEEE, Sep. 2023, pp. 1–6. doi: 10.1109/EMCEurope57790.2023.10274271.

[32] G. Fellner, S. Buttinger, D. Pommerenke, S. Shinde, and M. Hillstrom, “Statistical Characterization of Human-Induced ESD,” IEEE Trans Electromagn Compat, 2025.

Gabriel Fellner received his M.Sc. degree in electrical engineering in 2021 from Graz University of Technology, Graz, Austria, where he is currently working towards a Ph.D. degree in the field of electrostatic discharge. His research interests include methods for detection and quantification of ESD in real-world environments.

Simon Buttinger received his B.Sc. degree in electrical engineering in 2023 from Graz University of Technology, Graz, Austria, where he is currently pursuing a master’s degree in electrical engineering and business. He works as a student project assistant in ESD research.

David Pommerenke (F'15) received his Diploma and PhD from the Technical University Berlin, Germany. His research interests include EMC, ESD, electronics, numerical simulations, measurement methods and instrumentations. After working at Hewlett Packard for 5 years, he joined the Electromagnetic Compatibility Laboratory at the Missouri University of S&T in 2001. In 2020 he moved to Graz, Austria to join the Graz EMC lab at the Graz University of Technology. Most of his research is devoted to system level Electrostatic Discharge and EMC. He has published more than 150 journal papers and is an inventor on 13 patents. He is IEEE Fellow and an associated editor of the TEMC.

Satyajeet Shinde received the B.E. degree in electronics and telecommunications engineering from the Savitribai Phule Pune University, Pune, India, in 2010, and the M.S. and Ph.D. degrees in electrical engineering from the Missouri University of Science and Technology, Rolla, MO, USA, in 2014 and 2017, respectively. He was a Graduate Research Assistant with the Electromagnetic Compatibility Laboratory, Missouri University of Science and Technology. He was a Signal Integrity Summer Intern with Micron Technology, Boise, ID, USA, in 2013, and an EMC Design Summer Intern with Apple, Cupertino, CA, USA, in 2015. He is currently working as an EMC Design Engineer at Apple (Cupertino, CA, USA). His research interests include intra-system RFI, radiated emission modeling techniques, EMC and ESD measurement methods, and RF system design.

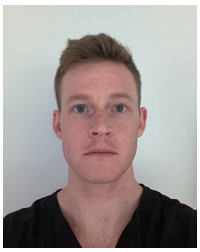

Michael Hillstrom is an EMC Design Engineering Manager at Apple. He received his bachelor's degree in electrical and computer engineering from the Missouri University of Science & Technology and master's degree in electrical engineering from Stanford University. He joined Apple as an EMC Design Engineer in 2013 and became a manager in 2021. He is interested in consumer electronics research and development with a focus on system design for ESD and EMI.